

# Uniaxial Strain Tuning of Upconversion Photoluminescence in Monolayer WSe<sub>2</sub>

Shrawan Roy, Xiaodong Yang, and Jie Gao\*

Strain engineering is one of the leading mechanical ways to tune the optical properties of monolayer transition metal dichalcogenides among different techniques. Here, uniaxial strain is applied on exfoliated 1L-WSe<sub>2</sub> flakes transferred on flexible polycarbonate substrates to study the strain tuning of upconversion photoluminescence. It is demonstrated that the peak position of upconversion photoluminescence is redshifted by around 20 nm as the applied uniaxial strain increases from 0% to 1.17%, while the intensity of upconversion photoluminescence increases exponentially for the upconversion energy difference ranging from  $-155$  to  $-32$  meV. The linear and sublinear power dependence of upconversion photoluminescence is observed for different excitation wavelengths with and without uniaxial strain, suggesting the multiphonon-assisted mechanism in one-photon regime for the upconversion process. These results offer the potential to advance 2D material-based optical upconversion applications in night vision, strain-tunable infrared detection, and flexible optoelectronics.

## 1. Introduction

Due to the formation of excitons and different excitonic complexes in monolayer transition metal dichalcogenides (1L-TMDs) even at room temperature, there have been highly perused atomically layered semiconductors in the field of optoelectronics since a decade.<sup>[1–5]</sup> Generally, photoluminescence (PL) has been observed in 1L-TMDs from the formed excitons along with complexes when they are excited by the photons with energy higher than the bandgap. On the other hand, upconversion photoluminescence (UPL) has also been observed in 1L-TMDs when excited by the photons with energy lower than

the bandgap at both low temperature and room temperature.<sup>[6–8]</sup> UPL is an anti-Stokes process in which the emitted photons have higher energy than the absorbed photons, and it has been demonstrated in different materials like quantum dots,<sup>[9]</sup> quantum wells,<sup>[10]</sup> organic dyes,<sup>[11,12]</sup> rare-earth-doped materials,<sup>[13]</sup> as well as 1L-TMDs.<sup>[6–8,14]</sup> This phenomenon plays an important role for broad applications in the fields of displays,<sup>[15]</sup> lasers,<sup>[16]</sup> bioimaging,<sup>[17,18]</sup> photovoltaic energy conversion,<sup>[19]</sup> and optical refrigeration.<sup>[20]</sup>


The optical properties of 1L-TMDs can be tuned by different approaches such as chemical treatment,<sup>[3,5,21–24]</sup> heterostructure forming,<sup>[2,4,25,26]</sup> electrostatic doping,<sup>[27–29]</sup> and strain engineering.<sup>[30–34]</sup> Strain engineering is one effective technique that changes crystal lattice and electronic band structure of TMDs with dif-

ferent thicknesses and thus modulates their optical responses like PL, Raman scattering, reflection, and absorption.<sup>[30–34]</sup> Specially, strain can be applied to TMDs by transferring TMDs on patterned substrates,<sup>[35,36]</sup> producing ripples and wrinkles in TMDs,<sup>[34,37]</sup> and bending TMDs on flexible substrates.<sup>[33,38]</sup> Strain-modulated UPL emission in TMDs is desired for promising applications in tunable photon upconversion devices and flexible optoelectronics. However, the study of strain tuning of UPL emission in TMDs has not been explored yet.

In this work, uniaxial strain-dependent UPL emission from mechanically exfoliated 1L-WSe<sub>2</sub> at room temperature is demonstrated. Uniaxial tensile strain up to 1.17% is applied on 1L-WSe<sub>2</sub> transferred on flexible polycarbonate (PC) substrate using a three-point bending strain apparatus. As the applied uniaxial strain on 1L-WSe<sub>2</sub> increases from 0% to 1.17%, the UPL peak position is redshifted by around 20 nm and the UPL intensity grows exponentially at the excitation wavelengths of 784, 800, and 820 nm. Strain tuning of UPL emission is demonstrated across broad range of the upconversion energy difference from  $-155$  to  $-32$  meV, together with two orders of magnitude enhancement of the integrated UPL emission intensity. Furthermore, the measured linear power dependence of UPL emission with and without uniaxial strain indicates that UPL in 1L-WSe<sub>2</sub> under uniaxial strain follows the multiphonon-assisted upconversion process in one-photon regime. Our results will advance many photon upconversion applications based on TMDs such as night vision, strain-tunable infrared detection, and flexible optoelectronics.

S. Roy, X. Yang  
Department of Mechanical and Aerospace Engineering  
Missouri University of Science and Technology  
Rolla, MO 65409, USA

J. Gao  
Department of Mechanical Engineering  
Stony Brook University  
Stony Brook, NY 11794, USA  
E-mail: jie.gao.5@stonybrook.edu

 The ORCID identification number(s) for the author(s) of this article can be found under <https://doi.org/10.1002/adpr.202300220>.

© 2023 The Authors. Advanced Photonics Research published by Wiley-VCH GmbH. This is an open access article under the terms of the Creative Commons Attribution License, which permits use, distribution and reproduction in any medium, provided the original work is properly cited.

DOI: 10.1002/adpr.202300220

## 2. Results and Discussion

Figure 1a illustrates the optical reflection microscope image of the exfoliated WSe<sub>2</sub> flakes transferred on PC substrate, where the 1L-WSe<sub>2</sub> area is highlighted with the dotted lines. The schematic diagram of the three-point bending strain apparatus for applying the uniaxial tensile strain on 1L-WSe<sub>2</sub> on PC substrate is displayed in Figure 1b. The applied uniaxial tensile strain  $\epsilon$  on 1L-WSe<sub>2</sub> due to the deflection of PC substrate is estimated as  $\epsilon = 6dt/l^2$ , where  $l$  is the distance between the two pivotal points ( $l = 25.4$  mm),  $t$  is the thickness of the PC substrate ( $t = 0.25$  mm), and  $d$  is the displacement of the two pivotal points.<sup>[33]</sup> Room-temperature PL spectra of 1L-WSe<sub>2</sub> excited at 633 nm at different uniaxial tensile strain levels are presented in Figure 1c. When there is no strain (0%), the peak position of PL spectrum is observed at 744 nm, which is consistent with the typical PL spectra of 1L-WSe<sub>2</sub>.<sup>[39,40]</sup> The PL peak position exhibits a wavelength redshift as the applied strain increases gradually from 0% to 1.17%. Figure 1e plots the PL peak position as a function of the applied strain, showing a linear redshift of 25.6 nm/% strain (55 meV/% strain), which is similar to the previous work.<sup>[41]</sup> Similarly, the strain-dependent Raman characterization of 1L-WSe<sub>2</sub> is presented in Figure 1d,f. The Raman spectrum of 1L-WSe<sub>2</sub> at 0% strain shows the peak position at  $\approx 250$  cm<sup>-1</sup> for the degenerated in-plane E<sub>2g</sub><sup>1</sup> phonon mode and out-of-plane A<sub>1g</sub> phonon mode, which is consistent with the typical Raman spectra of 1L-WSe<sub>2</sub>.<sup>[2,14]</sup> The peak position of Raman spectra continuously redshifts with the increased

strain and a 2.2 cm<sup>-1</sup> shift is observed under 1.02% applied strain compared to the case without strain, resulting from the strain-induced crystal symmetry breaking and vibration softening.<sup>[34,42]</sup> The linear dependence of the Raman peak position on the applied strain is shown in Figure 1f, giving a redshift of 2.16 cm<sup>-1</sup>/% strain. It is noted that the slightly blueshifted Raman peak position at 1.17% strain compared to 1.02% strain may be due to the reduction in attachment of the 1L-WSe<sub>2</sub> on PC substrate after applying multiple cycles of strain.

The strain-dependent UPL spectra of 1L-WSe<sub>2</sub> excited at 784, 800, and 820 nm are shown in Figure 2a–c respectively. When there is no strain applied, the UPL spectra of 1L-WSe<sub>2</sub> show the peak position at  $\approx 744$  nm under all excitation wavelengths, which match the measured PL peak position of 1L-WSe<sub>2</sub> in Figure 1c. As the strain level is increased from 0% to 1.17%, UPL peak position is redshifted caused by the reduced bandgap under strain. Meanwhile, UPL emission intensity is significantly enhanced by 5, 6, and 4 folds under the excitation wavelength of 784, 800, and 820 nm, respectively, due to the continuously reduced energy difference between excitation and emission. It is noted that the full range of UPL spectra is not provided at the excitation of 784 and 800 nm due to the use of a 775 nm shortpass filter. Figure 3a presents the UPL peak position as a function of the applied strain under different excitation wavelengths, which shows the linear dependence of the redshifted peak position on the increased strain. It is found that the redshift of 24, 18, and 17 nm is observed under 1.17% applied strain compared to the case without strain at the excitation wavelength of

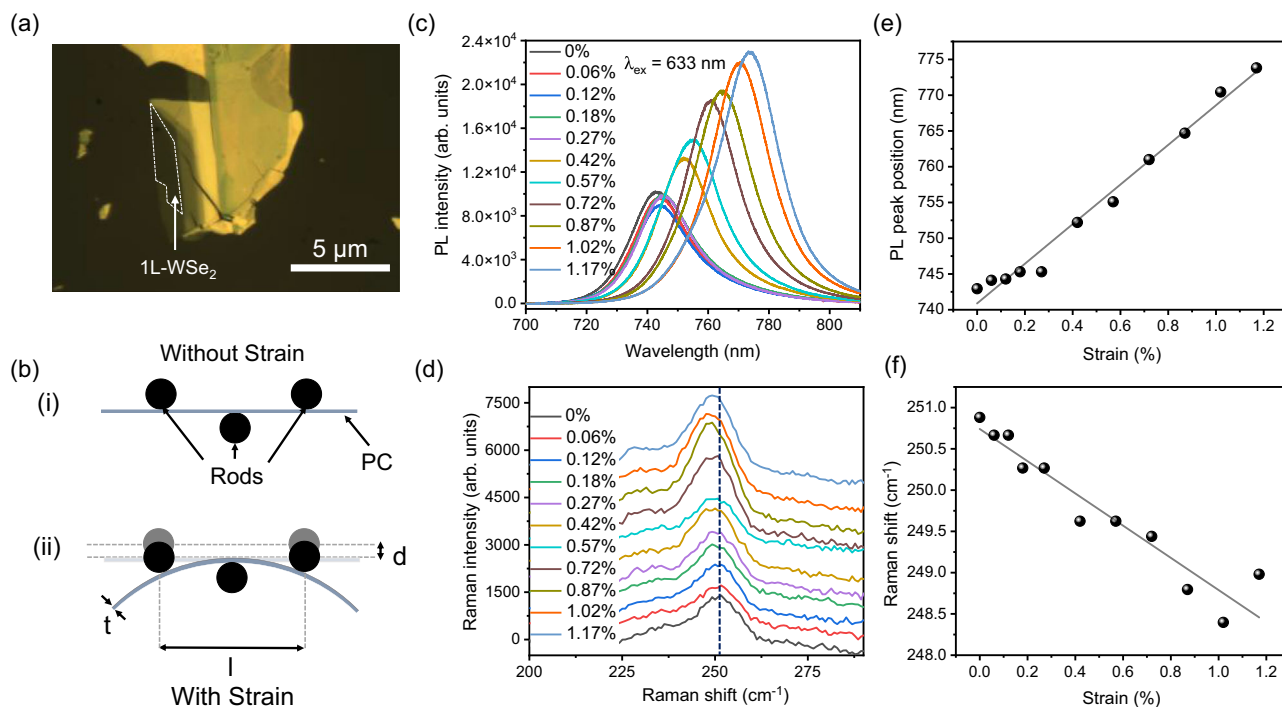


**Figure 1.** a) Optical reflection microscope image of the exfoliated WSe<sub>2</sub> flakes transferred on PC substrate. 1L-WSe<sub>2</sub> area is highlighted with the dotted lines. Scale bar is 5  $\mu$ m. b) Schematic diagram of the three-point bending strain apparatus. Strain-dependent c) PL and d) Raman spectra of 1L-WSe<sub>2</sub> excited at 633 nm at different uniaxial tensile strain levels. Peak positions of e) PL and f) Raman spectra as a function of the applied strain. Gray lines show the linear fittings.

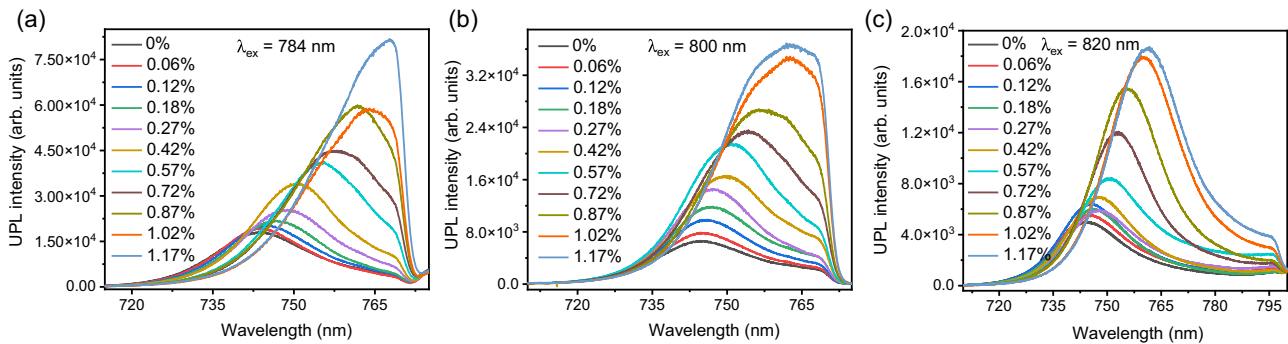


**Figure 2.** Strain-dependent UPL spectra of 1L-WSe<sub>2</sub> at the excitation wavelength of a) 784 nm, b) 800 nm, and c) 820 nm, respectively.

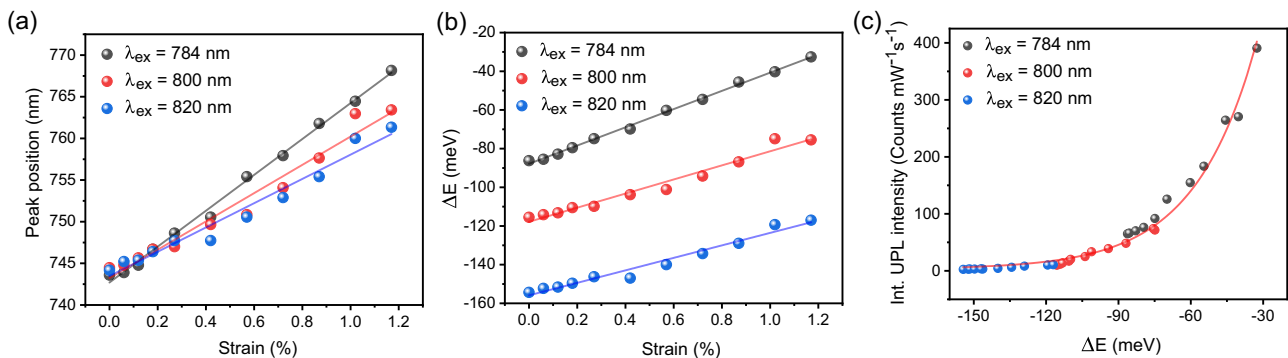


**Figure 3.** a) UPL peak position versus the applied strain at the excitation wavelength of 784, 800, and 820 nm. b) Strain-tunable energy difference  $\Delta E$  at three excitation wavelengths. c) Integrated UPL intensity as a function of  $\Delta E$ . Solid line shows the Boltzmann function fitting at room temperature.

784, 800, and 820 nm, respectively, giving the average redshift of around 20 nm. The average strain tuning gauge factor of the UPL peak position under all excitation wavelengths is around 17 nm/% strain (37 meV/%), while the slight difference of the linear slopes is due to the variation of the attachment condition between the 1L-WSe<sub>2</sub> and the PC substrate during multiple strain loading cycles. Figure 3b illustrates the energy difference between the excitation photon energy and the UPL emission energy  $\Delta E = \hbar\omega_{\text{exc}} - \hbar\omega_{\text{UPL}}$  as a function of the applied strain on 1L-WSe<sub>2</sub> for all three excitation wavelengths at room temperature. It shows that strain-tunable  $\Delta E$  for the upconversion process is achieved from  $-86$  to  $-32$  meV at the excitation of 784 nm,  $-115$  to  $-75$  meV at 800 nm, and  $-155$  to  $-117$  meV at 820 nm, respectively. Overall, a broad upconversion energy difference  $\Delta E$  ranging from  $-155$  to  $-32$  meV is realized. As  $\Delta E$  is continuously tuned, the integrated UPL intensity grows exponentially with two orders of magnitude enhancement, as shown in Figure 3c. The integrated UPL intensity follows the Boltzmann function  $I_{\text{UPL}} \propto \exp(-|\Delta E|/k_B T)$  where  $|\Delta E|$  is the upconversion energy gain,  $k_B$  is the Boltzmann constant, and room temperature  $T = 298$  K. It is worth mentioning that the observed UPL emission with below-bandgap excitation is mediated by the absorption of multiple phonons then followed by the carrier relaxation to the band edge and the exciton recombination. The origin of initial states could be from the trion tail with significantly broadened absorption features at room temperature.<sup>[8]</sup> For the multiphonon-assisted UPL emission in 1L-WSe<sub>2</sub>, the

involved effective phonon number in the upconversion process is approximately estimated from 5 to 1 as  $\Delta E$  varies from  $-155$  to  $-32$  meV, according to the optical phonon energy of 31 meV for 1L-WSe<sub>2</sub>.

The power-dependent UPL spectra excited at 820 nm with 0% strain and 0.8% strain are shown in Figure 4a,c, where the UPL intensity increases gradually with the excitation power while the UPL spectral shape is maintained. Figure 4b,d shows the integrated intensities of PL and UPL emission from 1L-WSe<sub>2</sub> excited at 633, 784, 800, and 820 nm in a log-log scale. The measured power-dependent emission intensities are fit with the power law  $I = \alpha P^\beta$ , where  $P$  is the excitation power,  $\alpha$  is the fitting parameter, and  $\beta$  is the exponent of the power law. When there is no strain applied, it can be seen from Figure 4b that the fit  $\beta$  values for UPL emission are very close to one for all excitation wavelengths, while PL emission exhibits a sublinear power dependence due to the saturated absorption. When there is 0.8% strain applied as shown in Figure 4d, a sublinear power dependence is observed at the excitation wavelengths of 784 and 800 nm, while an almost linear power dependence is exhibited at 820 nm. The  $\beta$  value decreases as the excitation wavelength gets shorter and closer to the UPL emission wavelength. The sublinear power dependence and  $\beta$  value changes observed for UPL emission may be related to the change of densities of phonons and exciton complexes.<sup>[8]</sup> The observed sublinear and linear dependence of UPL emission on the excitation power for 1L-WSe<sub>2</sub> with and without strain suggests that the UPL follows

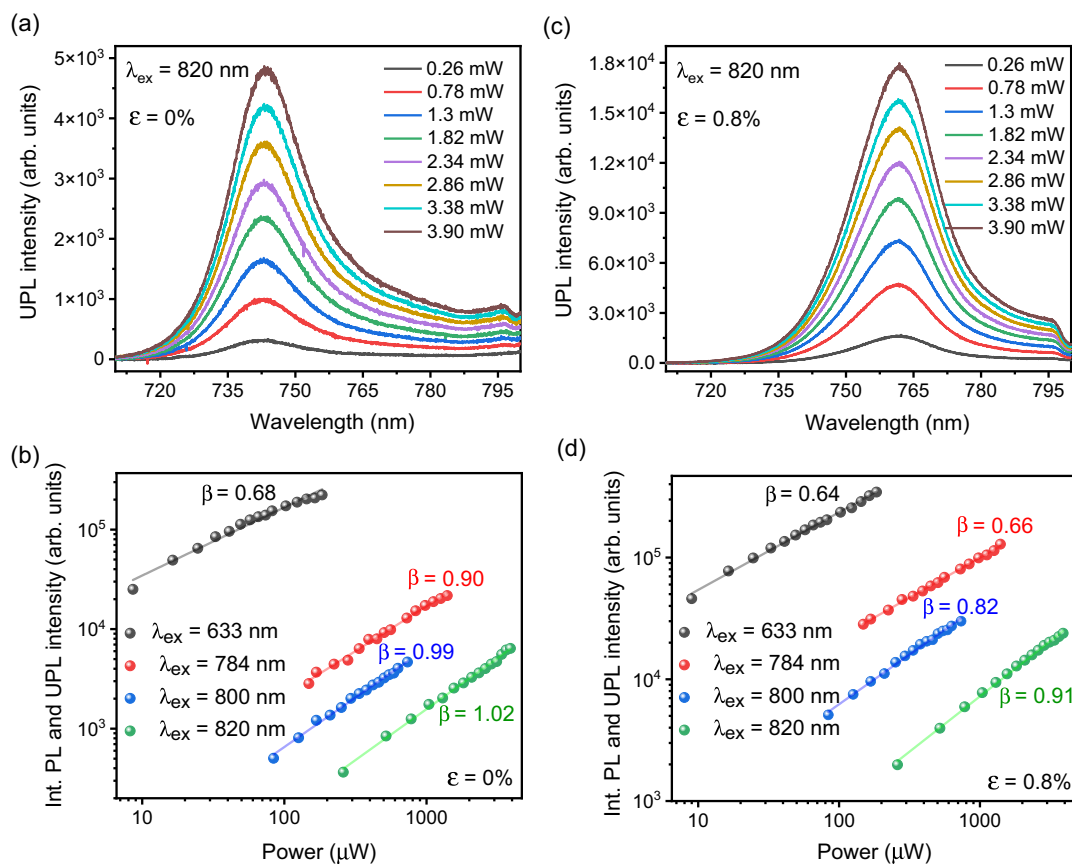


**Figure 4.** Power-dependent UPL spectra excited at 820 nm with a) 0% strain and c) 0.8% strain. Integrated intensities of PL and UPL emission in 1L-WSe<sub>2</sub> excited at 633, 784, 800, and 820 nm in a log–log scale with b) 0% strain and d) 0.8% strain.

a one-photon involved multiphonon-assisted upconversion process, ruling out the possibility of nonlinear optical effects like two-photon absorption or Auger recombination.

### 3. Conclusion

We have demonstrated uniaxial strain-dependent UPL emission in exfoliated 1L-WSe<sub>2</sub> on flexible substrate using a three-point bending strain apparatus at room temperature. Under different excitation wavelengths of 784, 800, and 820 nm, the peak position of UPL emission is redshifted by around 20 nm under the applied uniaxial strain up to 1.17%, while the UPL intensity grows exponentially as the strain increases. It is shown that two orders of magnitude increase of UPL intensity is achieved with strain-tuned upconversion energy difference from –155 to –32 meV. The observed linear and sublinear power dependence of UPL emission in 1L-WSe<sub>2</sub> with and without uniaxial strain indicates the UPL emission is a multiphonon-assisted upconversion process in one-photon regime. It is noteworthy that our study employs externally applied mechanical strain in TMDs on flexible substrate for the strain engineering of UPL enhancement. Strain engineering can also be adopted for photon upconversion in other material systems such as lanthanide-doped ferroelectric thin films grown on different

lattice-mismatched substrates.<sup>[43]</sup> In addition, interlayer rotation angle in TMD twisted bilayers can also be utilized as a tuning knob for modulating the UPL emission.<sup>[44]</sup> We envision that our results will open new opportunities in the development of tunable photon upconversion devices based on TMDs for future applications in night vision, infrared sensing, photodetection, and flexible optoelectronics.

### 4. Experimental Section

1L-WSe<sub>2</sub> flakes were mechanically exfoliated from a bulk WSe<sub>2</sub> crystal (2D Semiconductors) using scotch tape. For the typical process of sample preparation, bulk WSe<sub>2</sub> layers were directly deposited on scotch tape and exfoliated multiple times to get thinner layers, which were then gently placed on a piece of polydimethylsiloxane (PDMS) film on a glass slide for 45 min. Afterward, the tape was gently removed to get multilayer and monolayer WSe<sub>2</sub> flakes on PDMS, and 1L-WSe<sub>2</sub> flakes were confirmed by the microscopic image, PL, and Raman measurements. Then the exfoliated 1L-WSe<sub>2</sub> flakes on PDMS were transferred to the center of the rectangular PC substrate with the size of 15 mm by 65 mm and the thickness of 0.25 mm, where a dry transfer method based on an optical microscope facilitated with a micromanipulator was used.<sup>[45]</sup> Uniaxial tensile strain was applied to the 1L-WSe<sub>2</sub> on flexible PC substrate by three-point bending strain apparatus using three metallic rods as the pivotal points to control the deflection of PC substrate.<sup>[18]</sup> PL and Raman spectra of 1L-WSe<sub>2</sub> flakes on PC substrate were measured with a 633 nm He–Ne excitation laser by collecting the back-reflected signal through a 50× objective lens



(NA = 0.42) coupled into a spectrometer (Horiba, iHR 550). Similarly, UPL spectra were measured using the same experimental setup with continuous-wave excitation lasers at the wavelengths of 784, 800, and 820 nm and shortpass filters.

## Acknowledgements

The authors acknowledge support from the DARPA (grant no. W911NF2110353).

## Conflict of Interest

The authors declare no conflict of interest.

## Data Availability Statement

The data that support the findings of this study are available from the corresponding author upon reasonable request.

## Keywords

1L-WSe<sub>2</sub>, uniaxial strains, upconversion photoluminescence

Received: July 19, 2023

Revised: November 28, 2023

Published online:

- [1] K. F. Mak, C. Lee, J. Hone, J. Shan, T. F. Heinz, *Phys. Rev. Lett.* **2010**, *105*, 136805.
- [2] M. S. Kim, S. Roy, J. Lee, B. G. Kim, H. Kim, J. H. Park, S. J. Yun, G. H. Han, J.-Y. Leem, J. Kim, *ACS Appl. Mater. Interfaces* **2016**, *8*, 28809.
- [3] S. Roy, W. Choi, S. Jeon, D.-H. Kim, H. Kim, S. J. Yun, Y. Lee, J. Lee, Y.-M. Kim, J. Kim, *Nano Lett.* **2018**, *18*, 4523.
- [4] S. Roy, G. P. Neupane, K. P. Dhakal, J. Lee, S. J. Yun, G. H. Han, J. Kim, *J. Phys. Chem. C* **2017**, *121*, 1997.
- [5] K. P. Dhakal, S. Roy, S. J. Yun, G. Ghimire, C. Seo, J. Kim, *J. Mater. Chem. C* **2017**, *5*, 6820.
- [6] A. M. Jones, H. Yu, J. R. Schaibley, J. Yan, D. G. Mandrus, T. Taniguchi, K. Wantabe, H. Dery, W. Yao, X. Xu, *Nat. Phys.* **2016**, *12*, 323.
- [7] M. Manca, M. M. Glazov, C. Robert, F. Cadiz, T. Taniguchi, K. Wantabe, E. Courtade, T. Amand, P. Renucci, X. Marie, G. Wang, B. Urbaszek, *Nat. Commun.* **2017**, *8*, 14927.
- [8] J. Jadczyk, L. Bryja, J. Kutrowska-Girzycka, P. Kapuściński, M. Bieniek, Y.-S. Huang, P. Hawrylak, *Nat. Commun.* **2019**, *10*, 107.
- [9] Z. Deutsch, L. Neeman, D. Oron, *Nat. Nanotechnol.* **2013**, *8*, 649.
- [10] G. Bacher, C. Hartmann, H. Schweizer, T. Held, G. Mahler, H. Nickel, *Phys. Rev. B* **1993**, *47*, 9545.
- [11] J. Zhao, S. Ji, H. Guo, *RSC Adv.* **2011**, *1*, 937.
- [12] S. Balushev, T. Miteva, V. Yakutkin, G. Nelles, A. Yasuda, G. Wegner, *Phys. Rev. Lett.* **2006**, *97*, 143903.
- [13] F. Auzel, *Chem. Rev.* **2004**, *104*, 139.
- [14] A. Mushtaq, X. Yang, J. Gao, *Opt. Express* **2022**, *30*, 45212.
- [15] E. Downing, L. Hesselink, J. Ralston, R. Macfarlane, *Science* **1996**, *273*, 1185.
- [16] G. S. He, P. P. Markowicz, T.-C. Lin, P. N. Prasad, *Nature* **2002**, *415*, 767.
- [17] C. Vinegoni, D. Razansky, S. A. Hilderbrand, F. Shao, V. Ntziachristos, R. Weissleder, *Opt. Lett.* **2009**, *34*, 2566.
- [18] C. T. Xu, N. Svensson, J. Axelsson, P. Svenmarker, G. Somesfalean, G. Chen, H. Liang, H. Liu, Z. Zhang, S. Andersson-Engels, *Appl. Phys. Lett.* **2008**, *93*, 171103.
- [19] V. Gray, D. Dzebo, M. Abrahamsson, B. Albinsson, K. Moth-Poulsen, *Phys. Chem. Chem. Phys.* **2014**, *16*, 10345.
- [20] R. I. Epstein, M. I. Buchwald, B. C. Edwards, T. R. Gosnell, C. E. Mungan, *Nature* **1995**, *377*, 500.
- [21] M. Amani, D.-H. Lien, D. Kiriya, J. Xiao, A. Azcatl, J. Noh, S. R. Madhvapathy, R. KC, S. Addou, M. Dubey, K. Cho, R. M. Wallace, S.-C. Lee, J.-H. He, J. W. Ager III, X. Zhang, E. Yablonovitch, A. Javey, *Science* **2015**, *350*, 1065.
- [22] S. Mouri, Y. Miyauchi, K. Matsuda, *Nano Lett.* **2013**, *13*, 5944.
- [23] H.-V. Han, A.-Y. Lu, L.-S. Lu, J.-K. Huang, H. Li, C.-L. Hsu, Y.-C. Lin, M.-H. Chiu, K. Suenaga, C.-W. Chu, H.-C. Kuo, W.-H. Chang, L.-J. Li, Y. Shi, *ACS Nano* **2016**, *10*, 1454.
- [24] W. Su, H. Dou, J. Li, D. Huo, N. Dai, L. Yang, *RSC Adv.* **2015**, *5*, 82924.
- [25] M. S. Kim, C. Seo, H. Kim, J. Lee, D. H. Luong, J.-H. Park, G. H. Han, J. Kim, *ACS Nano* **2016**, *10*, 6211.
- [26] S. Roy, M.-H. Doan, J. Kim, S. K. Kang, G. H. Ahn, H. S. Lee, S. J. Yun, J. Kim, *J. Korean Phys. Soc.* **2021**, *78*, 693.
- [27] K. F. Mak, K. He, C. Lee, G. H. Lee, J. Hone, T. F. Heinz, J. Shan, *Nat. Mater.* **2013**, *12*, 207.
- [28] J. S. Ross, S. Wu, H. Yu, N. J. Ghimire, A. M. Jones, G. Aivazian, J. Yan, D. G. Mandrus, D. Xiao, W. Yao, X. Xu, *Nat. Commun.* **2013**, *4*, 1474.
- [29] S. Tongay, J. Zhou, C. Ataca, J. Liu, J. S. Kang, T. S. Matthews, L. You, J. Li, J. C. Grossman, J. Wu, *Nano Lett.* **2013**, *13*, 2831.
- [30] S. B. Desai, G. Seol, J. S. Kang, H. Fang, C. Battaglia, R. Kapadia, J. W. Ager, J. Guo, A. Javey, *Nano Lett.* **2014**, *14*, 4592.
- [31] W. Wu, J. Wang, P. Ercius, N. C. Wright, D. M. Leppert-Simenaer, R. A. Burke, M. Dubey, A. M. Dogare, M. T. Pettes, *Nano Lett.* **2018**, *18*, 2351.
- [32] J. O. Island, A. Kuc, E. H. Diependaal, R. Bratschkitsch, H. S. J. Van der Zant, T. Hiene, A. Castellanos-Gomez, *Nanoscale* **2016**, *8*, 2589.
- [33] F. Carrascoso, H. Li, R. Frisenda, A. Castellanos-Gomez, *Nano Res.* **2021**, *14*, 1698.
- [34] K. P. Dhakal, S. Roy, H. Jang, X. Chen, W. S. Yun, H. Kim, J. D. Lee, J. Kim, J.-H. Ahn, *Chem. Mater.* **2017**, *29*, 5124.
- [35] H. Li, A. W. Contryman, X. Qian, S. M. Ardakani, Y. Gong, X. Wang, J. M. Weisse, C. H. Lee, J. Zhao, P. M. Ajayan, H. C. Manoharan, X. Zheng, *Nat. Commun.* **2015**, *6*, 7381.
- [36] J. Chaste, A. Missaoui, S. Huang, H. Henck, Z. B. Aziza, L. Ferlazzo, C. Naylor, A. Balan, A. T. C. Johnson Jr., R. Braive, A. Ouerghi, *ACS Nano* **2018**, *12*, 3235.
- [37] J. Wang, M. Han, Q. Wang, Y. Ji, X. Zhang, R. Shi, Z. Wu, L. Zhang, A. Amini, L. Guo, N. Wang, J. Lin, C. Cheng, *ACS Nano* **2021**, *15*, 6633.
- [38] F. Carrascoso, R. Frisenda, A. Castellanos-Gomez, *Nano Mater. Sci.* **2022**, *4*, 44.
- [39] N. Mondal, N. Azam, Y. N. Gartstein, M. Mahjouti-Samani, A. V. Malko, *Adv. Mater.* **2022**, *34*, 2110568.
- [40] X. Chen, Z. Wang, L. Wang, H.-Y. Wang, Y.-Y. Yue, H. Wang, X.-P. Wang, A. T. S. Wee, C.-W. Qiu, H.-B. Sun, *Nanoscale* **2018**, *10*, 9346.
- [41] B. Aslan, M. Deng, T. F. Heinz, *Phys. Rev. B* **2018**, *98*, 115308.

- [42] A. Castellanos-Gomez, R. Roldan, E. Cappelluti, M. Buscema, F. Guinea, H. S. J. Van der Zant, G. A. Steele, *Nano Lett.* **2013**, *13*, 5361.
- [43] S. Li, H. Chen, Y. Zhao, Z. Chen, E.-J. Guo, Z. Wu, Y. Zhang, W. Tang, K. K. Kim, J. Hao, *J. Phys. D: Appl. Phys.* **2019**, *52*, 234002.
- [44] Y. Dai, P. Qi, G. Tao, G. Yao, B. Shi, Z. Liu, Z. Liu, X. He, P. Peng, Z. Dang, L. Zheng, T. Zhang, Y. Gong, Y. Guan, K. Liu, Z. Fang, *Light Sci. Appl.* **2023**, *12*, 6.
- [45] Q. Zhao, T. Wang, Y. K. Ryu, R. Frisenda, A. J. Castellanos-Gomez, *J. Phys. Mater.* **2020**, *3*, 016001.